P-ISSN 2586-9000
E-ISSN 2586-9027
Homepage : https://tci-thaijo.org/index.php/SciTechAsia
Science & Technology Asia
Vol.27 No.2 April - June 2022
Page: [69-77]
Original research article

Entropy Generation During MHD Fluid Flow of Viscoelastic Fluid Through a Deformable Porous Layer

Utpal Jyoti Das[1,*], Mira Das[2]

[1]*Department of Mathematics, Gauhati University, Guwahati 781014, India*
[2]*Department of Mathematics, Rajiv Gandhi University, Doimukh 791112, India*

Received 23 November 2020; Received in revised form 28 April 2021
Accepted 12 May 2021; Available online 29 June 2022

ABSTRACT

The problem of magnetohydrodynamic (MHD) flow of viscoelastic fluid in a deformable vertical porous layer with entropy generation analysis has been investigated. The vertical walls are subjected to a constant injection/suction velocity. The expressions for solid displacement, fluid velocity and temperature distribution are derived. The impact of relevant parameters on the solid displacement, fluid velocity, temperature, entropy generation number and Bejan number are discussed graphically.

Keywords: Bejan number; Deformable porous layer; Entropy generation number; MHD; Viscoelastic fluid

1. Introduction

The study of viscous fluid flow through deformable porous material has been studied by many researchers due to its wide applications in the fields of engineering, biological problems of skin and tissue mechanics for articular cartilage. Terzaghi [1] initiated the study of deformation of porous materials and fluid movement. Biot [2] developed this theory of deformation and acoustic propagation of fluid. This model is used to study the permeability of arterial wall [3- 5] and articular cartilage [6-7]. Barry et al. [8] investigated the problem of viscous fluid in a channel of deformable porous material for the examination of the impact of glycocalyx on flow inside blood vessels. Ambrosi [9] studied the mechanics of infiltration over porous medium. Sreenadh et al. [10] studied Couette flow in a deformable bed. Sreenadh et al. [11-12] analyzed Jeffrey fluid flow over deformable porous layer. Murthy [13] studied the MHD Casson liquid flow over a deformable porous medium with slip effects.

The study of entropy generation in a system of fluid is an important part of heat transfer analysis and in its efficiency in performing. Bejan [14] explained the analysis of heat transfer in viscous fluid. Also, Bejan

***Corresponding author:** utpaljyotidas@yahoo.co.in **doi:** 10.14456/scitechasia.2022.25

[15] presented entropy generation analysis and heat transfer in fluid flow system. Eegunjobi and Makinde [16] studied the entropy generation of an MHD flow with variable viscosity in a channel. Das and Jana [17] studied entropy in a flow of an incompressible viscous fluid in a porous channel incorporating Navier slip condition. Sreenadh et al. [18] analyzed the entropy generation for MHD flow in a vertical deformable porous layer.

The above works have motivated us to study the MHD flow of viscoelastic fluid through a deformable porous layer with constant injection/ suction at the walls. Here, the aim is to investigate the effects of viscoelastic parameter and entropy generation analysis in MHD flow. The novelty of this work lies in the study of flow behavior of viscoelastic fluid in the case of a deformable porous layer.

2. Mathematical Formulation

Consider a steady MHD flow of an incompressible viscoelastic fluid, characterized by Walters' liquid model B' through a deformable, vertical porous layer with constant injection/suction velocity at the porous walls. The porous material is designed as a continuous, homogeneous and isotropic mixture of fluid and solid phases where each point in the binary mixture is occupied concurrently by fluid and solid. The $\bar{x}$ - axis is taken along the midway of the channel and $\bar{y}$ -axis at right angles to it as shown in Fig.1. The heat is generated in the fluid by viscous and Darcy dissipations. The walls of the channel are at a distance $2h$.

The governing equations of the flow, following Barry et al. [8] and Sreenadh et al. [12] for viscoelastic fluid become

$$\mu\frac{\partial^2\bar{u}}{d\bar{y}^2}+K\bar{v}-(1-\phi)\frac{\partial\bar{P}}{\partial\bar{x}}=0, \qquad (2.1)$$

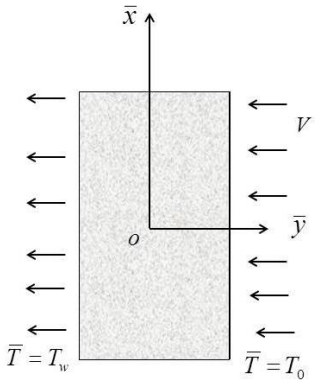

Fig. 1. Physical model of the problem.

$$V\bar{\gamma}\frac{\partial^3\bar{v}}{\partial\bar{y}^3}+2\mu_a\frac{\partial^2\bar{v}}{\partial\bar{y}^2}+\rho^f V\frac{\partial\bar{v}}{\partial\bar{y}}-\phi\frac{\partial\bar{P}}{\partial\bar{x}}$$
$$+g\rho^f\beta_T(\bar{T}-T_0)-K\bar{v}-\sigma B_0^2\bar{v}=0, \qquad (2.2)$$

$$K_0\frac{\partial^2\bar{T}}{\partial\bar{y}^2}+\rho^f C_p V\frac{\partial\bar{T}}{\partial\bar{y}}+K\bar{v}^2$$
$$-V\bar{\gamma}\frac{\partial\bar{v}}{\partial\bar{y}}\frac{\partial^2\bar{v}}{\partial\bar{y}^2}=0. \qquad (2.3)$$

The boundary conditions are

$$\bar{v}=0,\bar{u}=0,\bar{T}=T_0 \text{ at } \bar{y}=h;$$
$$\frac{d\bar{v}}{d\bar{y}}=0,\frac{d\bar{u}}{d\bar{y}}=0,\frac{d\bar{T}}{d\bar{y}}=0 \text{ at } \bar{y}=0, \qquad (2.4)$$

where $\bar{u},\bar{v}$ are velocity components along $\bar{x},\bar{y}$-axes, $\bar{P}$ is pressure, μ is Lame constant, ϕ is volume fraction component for fluid phase, ρ^f is fluid density, μ_a is apparent viscosity of fluid, V is constant suction/injection velocity, B_0 is strength of magnetic field, β_T is coefficient of heat transfer, σ is electrical conductivity, K is drag coefficient, K_0 is thermal conductivity, and $\bar{T}$ is temperature.

The following non-dimensional quantities are introduced:

$$y=\frac{\bar{y}}{h}, v=\frac{\bar{v}}{V}, u=\frac{\bar{u}\mu}{\mu_f V}, x=\frac{\bar{x}}{h}, \theta=\frac{\bar{T}-T_0}{T_w-T_0},$$
$$P^*=\frac{h\bar{P}}{\mu_f V}, \mathrm{Re}=\frac{Vh}{\upsilon_f}, P=\frac{dP^*}{dx}, \eta=\frac{\mu_f}{2\mu_a},$$
$$Gr=\frac{g\beta_T\rho^f h^2(T_h-T_0)}{\mu_f V}, Br=\frac{\mu_f C_p}{K_0(T_w-T_0)},$$
$$\gamma=\frac{\bar{\gamma}}{\rho^f h^2}, \mathrm{Pr}=\frac{\mu_f C_p}{K_0}, M=\frac{h^2\sigma B_0^2}{\mu_f\rho^f},$$
$$\delta=\frac{Kh^2}{\mu_f}. \qquad (2.5)$$

Using (2.5) in Eqs. (2.1)-(2.3), we get

$$\frac{d^2u}{dy^2}-(1-\phi)P+\delta v=0, \qquad (2.6)$$

$$\mathrm{Re}\eta\gamma\frac{d^3v}{dy^3}+\frac{d^2v}{dy^2}+\mathrm{Re}\eta\frac{dv}{dy}-\phi P\eta+GrT-(\delta+M)\eta v=0, \qquad (2.7)$$

$$\frac{d^2\theta}{dy^2}+\mathrm{Pr}\,\mathrm{Re}\frac{d\theta}{dy}-\gamma Br\,\mathrm{Re}\frac{dv}{dy}\frac{d^2v}{dy^2}=0, \qquad (2.8)$$

where Re is Reynolds number, Pr is Prandtl number, Br is Brinkman number, γ is viscoelastic parameter, Gr is thermal Grash of number, M is Hartman number. The boundary conditions are

$$u=0, v=0, \theta=1 \text{ at } y=1;$$
$$\frac{dv}{dy}=0, \frac{du}{dy}=0, \frac{d\theta}{dy}=0 \text{ at } y=0 \qquad (2.9)$$

The Eqs. (2.6)-(2.8) cannot be solved in closed form. As $\gamma<<1$ for small shear rate, so to solve these non-linear coupled equations, we can take

$$(u,v,\theta)=(u_0,v_0,\theta_0)+\gamma(u_0,v_0,\theta_0)+o(\gamma^2) \qquad (2.10)$$

Using (2.10) in (2.6)-(2.8) and neglecting the higher powers γ, we obtain the following system of equations

$$\frac{d^2u_0}{dy^2}-(1-\phi)P+\delta v_0=0, \qquad (2.11)$$

$$\frac{d^2v_0}{dy^2}+\mathrm{Re}\eta\frac{dv_0}{dy}-\phi P\eta+Gr\theta_0-(\delta+M)\eta v_0=0, \qquad (2.12)$$

$$\frac{d^2\theta_0}{dy^2}+\mathrm{Pr}\,\mathrm{Re}\frac{d\theta_0}{dy}-\mathrm{Re}\,Br\frac{d^2v_0}{dy^2}\frac{dv_0}{dy}=0, \qquad (2.13)$$

$$\frac{d^2u_1}{dy^2}+\delta v_1=0, \qquad (2.14)$$

$$\frac{d^2v_1}{dy^2}+\mathrm{Re}\eta\frac{dv_1}{dy}+\mathrm{Re}\eta\frac{d^3v_0}{dy^3}+Gr\theta_1-(\delta+M)\eta v_1=0, \qquad (2.15)$$

$$\frac{d^2\theta_1}{dy^2}+\mathrm{Pr}\,\mathrm{Re}\frac{d\theta_1}{dy}-\mathrm{Re}\,N\frac{dv_0}{dy}\frac{d^2v_0}{dy^2}=0, \qquad (2.16)$$

with boundary conditions

$$u_0=u_1=0, v_0=v_1=0, \theta_0=1, \theta_1=0 \quad \text{at } y=1;$$
$$\frac{du_0}{dy}=\frac{du_1}{dy}=0, \frac{dv_0}{dy}=\frac{dv_1}{dy}=0, \frac{d\theta_0}{dy}=\frac{d\theta_1}{dy}=0 \quad \text{at } y=0. \qquad (2.17)$$

Solving the Eqs. (2.11)-(2.16) with boundary conditions (2.17), we get

$$u_0=A_5\exp(-m_1y)+A_6\exp(-m_2y)+A_7y+A_8y^2+A_9, \qquad (2.18)$$

$$u_1=A_{28}\exp(-m_1y)+A_{29}\exp(-m_2y)+A_{30}\exp(-2m_1y)+A_{31}\exp(-2m_2y)$$

$$+A_{32}\exp(-m_1y-m_2y)$$
$$+A_{33}\exp(-\mathrm{Pr}\,\mathrm{Re}\,y)+A_{34}y^2+A_{35}y$$
$$+A_{36}, \qquad (2.19)$$

$$v_0=A_2\exp(-m_1y)+A_3\exp(-m_2y)+A_1, \qquad (2.20)$$

$$v_1=A_{18}\exp(-m_1y)+A_{19}\exp(-m_2y)$$
$$+A_{20}\exp(-2m_1y)+A_{21}\exp(-2m_2y)$$
$$+A_{22}\exp(-m_1y-m_2y)A_{23}\exp(-\mathrm{Pr}\,\mathrm{Re}\,y)$$
$$+A_{24}, \qquad (2.21)$$

$$\theta_0=1, \qquad (2.22)$$

$$\theta_1=A_{13}\exp(-2m_1y)+A_{14}\exp(-m_2y)$$
$$+A_{15}\exp(-m_1y-m_2y)+A_{16}\exp(-\mathrm{Pr}\,\mathrm{Re}\,y)$$
$$+A_{17}, \qquad (2.23)$$

where

$$m_1=\frac{\mathrm{Re}\,\eta+\sqrt{\mathrm{Re}^2\eta^2+4(M+\delta)\eta}}{2},$$

$$m_2=\frac{\mathrm{Re}\,\eta-\sqrt{\mathrm{Re}^2\eta^2+4(M+\delta)\eta}}{2},$$

and the constants $A_i\,(i=1\text{ to }36)$ are not presented here for brevity.

3. Entropy Generation

Following Das and Jana [17], the entropy generation for the fluid flow through a deformable porous layer is

$$E_G=\frac{K_0}{T_0^2}\left(\frac{d\bar{T}}{d\bar{y}}\right)^2+\frac{2\mu_a}{T_0}\left(\frac{d\bar{v}}{d\bar{y}}\right)^2+\frac{K}{T_0}v^2$$
$$+\frac{\gamma V}{T_0}\frac{d^2\bar{v}}{d\bar{y}^2}\frac{d\bar{v}}{d\bar{y}}. \qquad (3.1)$$

The non-dimensional form of the entropy generation number N_S is given as

$$N_S=\frac{T_1^2a^2E_G}{\kappa(T_w-T_1)^2}$$
$$=\left(\frac{d\theta}{dy}\right)^2+\frac{Br}{\Omega}\left[\left(\frac{dv}{dy}\right)^2+\delta v^2+\gamma\,\mathrm{Re}\frac{d^2v}{dy^2}\frac{dv}{dy}\right]$$
$$=N_1+N_2$$

where $N_1=\left(\frac{d\theta}{dy}\right)^2$ is entropy generation due to heat transfer, $N_2=\frac{Br}{\Omega}\left[\left(\frac{dv}{dy}\right)^2+\delta v^2+\gamma\,\mathrm{Re}\frac{d^2v}{dy^2}\frac{dv}{dy}\right]$ is entropy generation due to viscous and elasticity, and $\Omega=\frac{T_w-T_0}{T_0}$ is the dimensionless temperature difference.

The Bejan number is defined as $Be=\frac{N_1}{N_S}=\frac{1}{1+\Phi}$, where $\Phi=\frac{N_2}{N_1}$ is the irreversibility ratio.

4. Results and Discussion

Numerical computations are carried out with the following parameter values $\mathrm{Pr}=2, M=1, \mathrm{Re}=2, \eta=1, Br=1, \phi=0.5, P=-2, Gr=2, \gamma=0.2$. Figs. 2-5 represent the displacement profile u for various values of viscoelastic parameter γ, volume fraction parameter ϕ, drag parameter δ and Hartmann number M, respectively. Fig. 2 shows that the solid displacement profile decreases due to an increase in γ from $\gamma=0$ to $\gamma=0.3$ through $\gamma=0.1, 0.2$. The solid displacement profile for $\gamma=0$ corresponds to Newtonian fluid and $\gamma\neq0$ corresponds to viscoelastic fluid. Fig. 3 shows that the solid displacement profile decreases due to an increase in ϕ. Fig. 4 depicts that the u increases when the drag parameter δ increases from

$\delta = 0.2$ to $\delta = 0.8$ through $\delta = 0.4, 0.6$. Physically, it can be said that during the growth of porosity there is less solid to impede and thus solid displacement decreases due to less drag on solid components. Fig. 5 shows that the values of u decrease as the Lorentz force i.e., the Hartmann number M increases.

Figs. 6-9 represent the fluid velocity profile v for various values of viscoelastic parameter γ, volume fraction parameter ϕ, drag parameter δ and Hartmann number M, respectively. It is observed that the values v decrease due to an increase in γ, δ, M, while the reverse effect is seen for increase in ϕ.

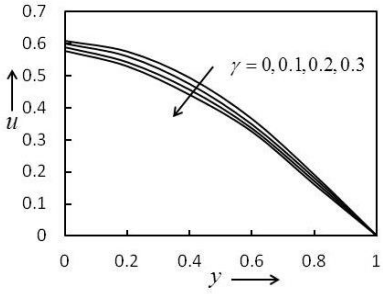

Fig. 2. Displacement profile for different γ.

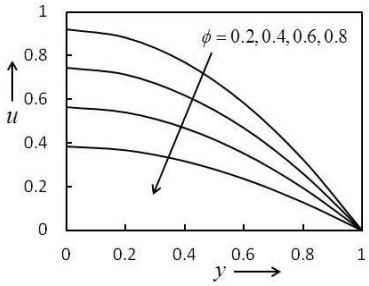

Fig. 3. Displacement profile for different ϕ.

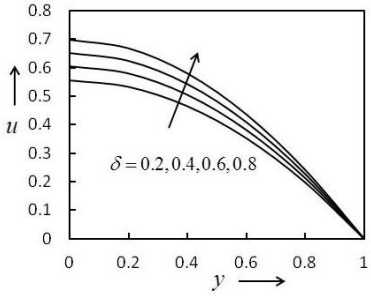

Fig. 4. Displacement profile for different δ.

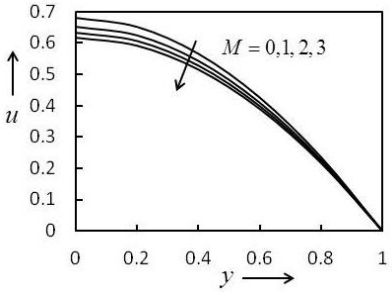

Fig. 5. Displacement profile for different M.

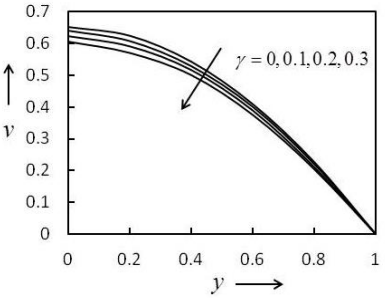

Fig. 6. Velocity profile for different γ.

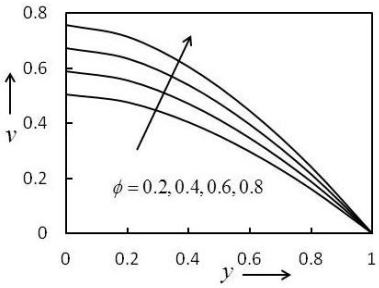

Fig. 7. Velocity profile for different ϕ.

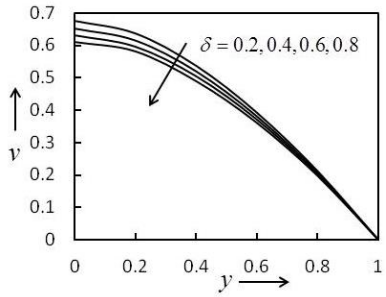

Fig. 8. Velocity profile for different δ.

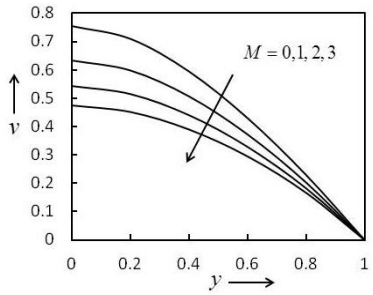

Fig. 9. Velocity profile for different M.

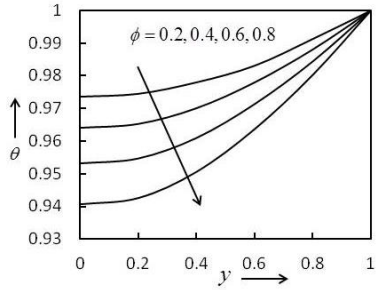

Fig. 10. Temperature profile for different ϕ.

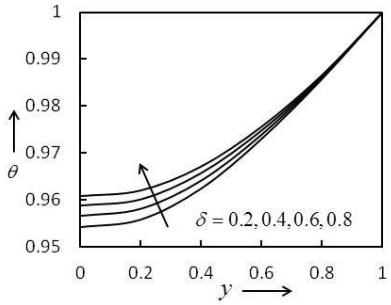

Fig. 11. Temperature profile for different δ.

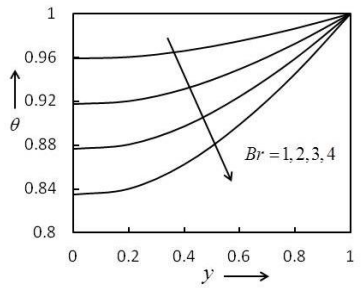

Fig. 12. Temperature profile for different Br.

Temperature profiles (θ) for different ϕ, δ, and Br are shown in Figs. 10-12. From Figs. 10 and 12 it is observed that temperature profiles decrease due to an increase in ϕ and Br while they increase when drag parameter δ increases (Fig. 11). Figs. 13-14 represent the entropy generation number and Bejan number for various.

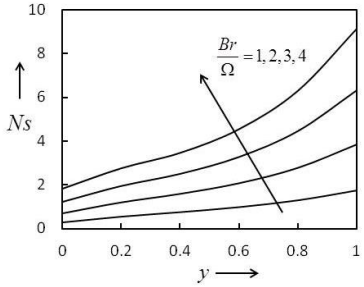

Fig. 13. Entropy generation number for different $\frac{Br}{\Omega}$.

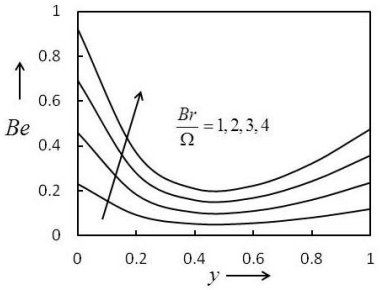

Fig. 14. Bejan number for different $\frac{Br}{\Omega}$.

values of $\frac{Br}{\Omega}$. It is observed that both the entropy generation number and Bejan number increase with the increase in $\frac{Br}{\Omega}$. Also, from Fig. 13 it is seen that the entropy generation number increases with the increase in y from $y=0$ to the wall $y=1$, while Fig. 14 shows that the Bejan number decreases with the increase in y from $y=0$ to $y=0.5$ (nearly). After that the Bejan number again increases for $y=0.5$ (nearly) to $y=1$.

Figs. 15-16 show the impact of γ on entropy generation number and Bejan number. It is observed that due to an increase in viscoelastic parameter γ from $\gamma=0$ to $\gamma=0.3$ through $\gamma=0.1,0.2$

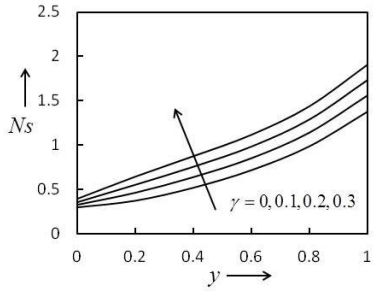

Fig. 15. Entropy generation number for different γ.

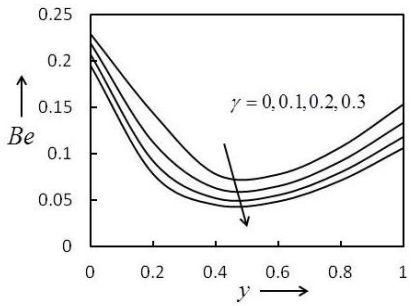

Fig. 16. Bejan number for different γ.

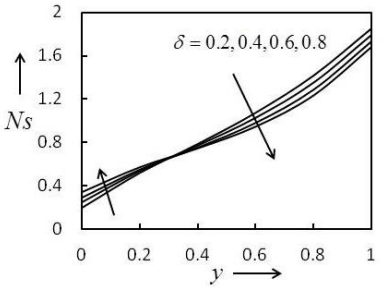

Fig. 17. Entropy generation number for different δ.

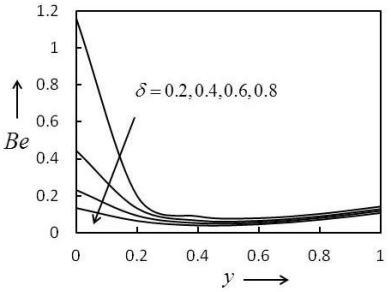

Fig. 18. Bejan number for different δ.

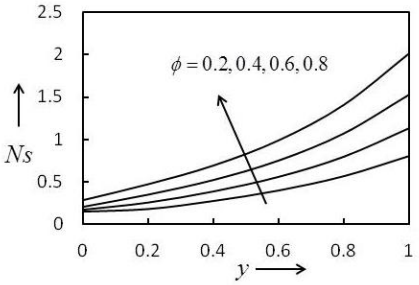

Fig. 19. Entropy generation number for different ϕ.

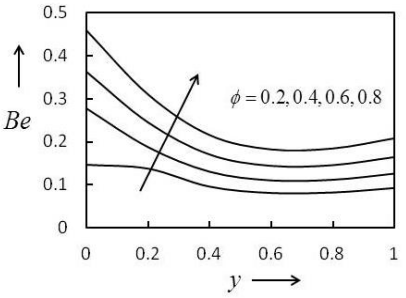

Fig. 20. Bejan number for different ϕ.

entropy generation numbers increase while Bejan number decreases. Figs. 17 -18 show the impact of δ on the entropy generation number and Bejan number. From Fig. 17 it is observed that the entropy generation number increases due to an increase in δ for $y = 0$ to $y = 0.3$ (nearly), but the reverse effect is seen for $y \in (0.3,1]$. Figure 18 shows that the Bejan number decreases due to an increase in δ. Figs. 19-20 show the impact of ϕ on entropy generation number and Bejan number. It is observed that both entropy generation number and Bejan number increase when the values of ϕ increase.

5. Conclusions

The above study led to the following conclusions:

1. The displacement profile increases due to an increase in the drag parameter, while it decreases due to an increase in the viscoelastic parameter, volume fraction parameter, and Hartmann number.
2. The fluid velocity profile increases due to an increase in the volume fraction parameter, while it decreases due to an increase in viscoelastic parameter, drag parameter, and Hartmann number.
3. The temperature profile decreases due to an increase in the volume fraction parameter and Brinkman number, while it increases when the drag parameter increases.
4. The entropy generation number increases with the increase in $\frac{Br}{\Omega}$, the viscoelastic parameter and volume fraction parameter.
5. The Bejan number increases with the increase in $\frac{Br}{\Omega}$ and volume fraction parameter, while it decreases when the viscoelastic parameter and drag parameter increase.

References

[1] Terzaghi K. Erdbaumechanik auf Bodenphysikalischen Grundlagen. Deuticke 1925.

[2] Biot MA. Mechanics of deformation and acoustic propagation in porous media. J Appl Phys. 1956; 27:240-53.

[3] Kenyon DE. A mathematical model of water flux through aortic tissue. Bull Math Biology. 1979; 41:79-90.

[4] Jayaraman G. Water transport in the arterial wall- A theoretical study. J Biomechanics, 1983; 16:833-40.

[5] Jain R, Jayaraman G. A theoretical model for water flux through the arterial wall. J Biomech Engng. 1987; 109:311-7.

[6] Holmes MH. A theoretical analysis for determining the nonlinear hydraulic permeability of a soft tissue from a permeation experiment, Bull Math Biology, 1985; 47:669-83.

[7] Holmes MH, Mow VC. The nonlinear characteristics of soft gels and hydrated connective tissue in ultra filtration. J Biomechanics. 1990; 23:1145-56.

[8] Barry SI, Parker KH, Aldis GK. Fluid flow over a thin deformable porous layer. J Appl Maths Phys. 1991; 42: 633-48.

[9] Ambrosi D. Infiltration through Deformable Porous Media. Z angew Math Mech. 2002; 82:115-24.

[10] Sreenadh S, Krishnamurthy M, Sudhakara M, Gopi Krishna G. Couette Flow over a deformable Bed. Int J innovat Res Sci Eng. 2014; 2:584-92.

[11] Sreenadh S, Krishnamurthy M, Sudhakara E, Gopi Krishna G, Venkateswarlu Naidu D. MHD free surface flow of a Jeffery fluid over a deformable

porous layer. Global journal of Pure and Applied Mathematics. 2015; 11(5): 3889-903.

[12] Sreenadh S, Rashidi MM, Kumara Swamy Naidu K, Parandhama, A. Free Convection Flow of a Jeffrey Fluid through a Vertical Deformable Porous Stratum. J Applied Fluid Mechanics. 2016; 9(5): 2391-401.

[13] Krishna Murthy M. Numerical investigation on magnetohydrodynamics flow of Casson fluid over a deformable porous layer with slip conditions. Indian J Phys. 2019; https://doi.org/10.1007/s12648-019-01668-4.

[14] Bejan A. Second law analysis in heat transfer and thermal design. Advances in heat transfer. 1982; 15:1-58.

[15] Bejan A. Entropy generation through heat transfer and fluid flow. Wiley, New York, 1982.

[16] Egnjobi AS, Makinde OD. Entropy generation analysis in a variable viscosity MHD channel flow with permeable walls and convective heating. Mathematical Problems in Engineering. 2013; http://dx.doi.org/10.1155/ 2013/630798.

[17] Das S, Jana RN. Entropy generation due to MHD flow in a porous channel with Navier slip. Ain Shams Engineering Journal. 2014; 5:575-84.

[18] Sreenadh S, Gopi Krishna G, Srinivas ANS, Sudhakara E. Entropy generation analysis for MHD flow through a vertical deformable porous layer. Journal of Porous Media. 2018; 21(6): 523-38.